

Comments to final submission (see individual comment in the 'reply' section)
 Marked up manuscript is attached at the end of the document

Reply to comments of RC1 and RC2

In the case that similar comments were done, I have grouped my reply to both.

Comments	Reply
<ul style="list-style-type: none"> I understand that it is not the purpose of the article to make a full literature review of the subject. However, this sound more like an excuse for not digging more into the pertinent literature. Nearly all reference and cited papers are related to own previous works. To justify publication, it is required more explicitly to argue the originality of the work and how it is inscribed in other literature and investigations. <p>Question 1: It is therefore important to have a literature review on the different control objectives in the field of wind energy (power control , load and fatigue ...) and the associated time scales (from large atmospheric boundary layer scales to small shear layer vortices or 3P ...). Authors should specify the objective study within this literature review. Also, in this review, it is certainly worth mentioning the only AFC using fluidic actuator (plasma actuator) work on a multi-MW turbine (Matsuda et al 2017), able to perform a very fast actuation (10kHz).</p> <p>H. Matsuda, M. Tanaka², T. Osako², K. Yamazaki¹, N. Shimura, M. Asayama and Y. Oryu "Plasma actuation effect on a MW class wind turbine" International Journal of Gas Turbine, Propulsion and Power Systems, February 2017, Volume 9, Number 1</p>	<p>Thank you for your comment, and I fully understand the concern. To keep the paper concise, the literature review focused initially solely on field experimental work on active flaps, which indeed is quite a limited field.</p> <p>In the revised version, I will include further the references, in particular to include the experimental wind tunnel work of Pechlivanoglou (TU Berlin), field work performed at the DTU on morphing flaps on a rotating test rig as a part of the InnWind project, and experimental work with trailing edge flaps of Samara and Johnson.</p> <p>As suggested by referee nr. 2, I will include the work of Matsuda et al, which I was aware of, but intendedly did not include it in the first revision of the paper as the focus is on plasma actuators and not on trailing edge flaps. In the updated revision of the paper I will include as it fits well with the experimental character of our submission</p> <p>Regarding the literature review of different control objectives as suggested by referee nr. 2, I think this is out of the scope of this paper. Control objectives for active devices on wind turbines is a very vast subject, both from the controller objective perspective, but also regarding the different devices (SJA, plasma, active gurneys, TE flaps, active leading edge, spoilers, blowing, suction, etc. It is the opinion of the authors that his field is already so wide, that a publication of experimental demonstration character such as the one we are proposing should not try to cover the literature of controller objectives.</p> <p>It is important for the authors to highlight, that the purpose of the work shown in our publication and also the work which was presented at the conference is focused on an experimental demonstration and testing of a system, but not the test of a particular controller strategy.</p>

	<p>Comments to final revision:</p> <p>The literature mentioned in my comment above has been included in the review, including also several contributions from the latest IEA Task 11 Expert Meeting on Smart Blades. The literature suggested by the reviewer has also been included.</p>
<ul style="list-style-type: none"> In the paper we learn that there is an effect of using active flaps, and that this effect indeed can be measured through the flapwise root moment. However, as we can see on Fig. 4 there is also a price to pay with respect to aerodynamic efficiency at high angles of attack. I think this balance between enhanced aeroelastic features vs the changed aerodynamics should be discussed. Furthermore, a general discussion of the motivation for using the flaps and a discussion of the potential gain of the achieved results are required, like, is a potential load impact of 5-10 % worthwhile of going after? 	<p>The discussion of lower aerodynamic efficiency is for sure a very interesting one. The full aero efficiency of the turbine can not be boiled down to the gliding ratio only, but depends also on the mean induction levels of the blade, the blade design strategy, and the operation strategy in the region around the shoulder of the power curve (where the performance is more sensitive to lift levels than to the lift to drag ratio. I will comment this balance of load handling vs. aerodynamic performance in a concise manner. To give an example, in the case of modern large offshore blades where the outboard area is designed towards low induction in order to allow for platform upscaling and where the AEP is geared towards high mean wind speeds, a penalty in lift over drag is overshadowed by the ability of increasing the induction level via lift levels. On the contrary, a smaller onshore turbine where the blades are designed for operation at lower mean wind speeds, the penalty of the lower gliding ratio will be more significant and may overshadow the ability to have the desired control authority from the active flaps. This is just to say that this is not a black or white discussion 😊</p> <p>Having a potential load handle of 5-10% is indeed worth going for and this was not clearly stated in the paper. From an industry perspective, load reductions can not be translated into LCOE in a direct manner on an existing platform and a cost-out of an existing turbine would not be the correct way to go, as the overhead costs would overshadow the improvement in LCOE. Therefore, such a load handle can be used in two ways: the first one is during the design phase of a new platform in order to enable a more cost effective dimensioning of the main components, and the second one (which is economically more attractive) is to upscale</p>

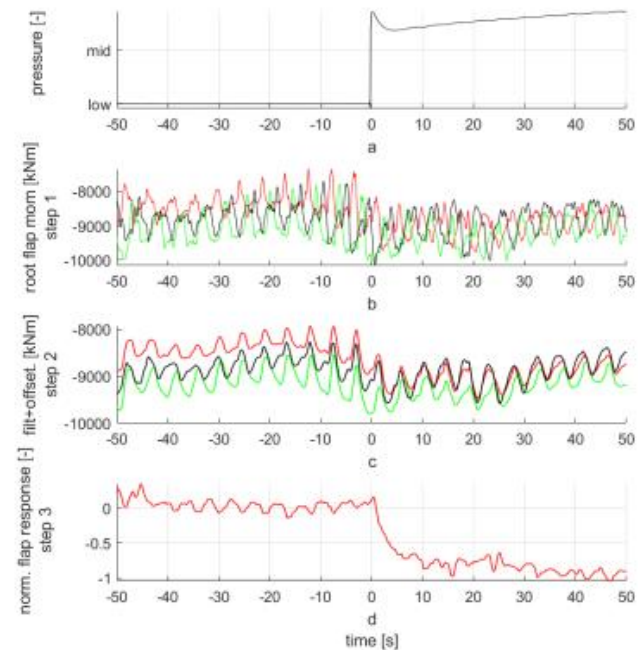
the rotor and maintaining the load envelope à this option has the higher impact on LCOE.

Comments to final revision:

A comment has been made to both items. This has been included in an additional section "3.4 discussion of results".

- Legends explaining the colors in Fig.6 are missing.

I will add these. In the plots with more than one time series (the two middle plots), each of them corresponds to the flapwise bending moment of one of the blades A, B, and C, and in the last plot, the loading corresponds to that of blade A after having applied the blade to blade comparison method (i.e. relative to blades B and C). These legends will be added



Comments to final revision:

All plots were labelled as described above

- Besides being limited to own research work, the citations and reference list is incomplete. On page 11 there are references to Fisker (2011) and Enevoldsen (2018) that do not appear in the reference list.

The comment to the references is addressed in the first point of the reply.

The references to Enevoldsen and Fisker are included, but I can see that there are two typos. In the reference to Peder Enevoldsen I wrote 2014 instead of 2018. In the reference to Peter Skjoldan Fisker I used his middle name (Fisker) instead of his last name (Skjoldan) when referencing it in the text. I will correct this.

Enevoldsen, P.B.: Load validation and advanced modelling. Advances in Rotor Blades for Wind Turbines - IQPC Conference, April 24-26 2018, Bremen, Germany, 2018.
 Energiteknologiske Udviklings- og Demonstrationsprogram. Project Journal Nr. 64015-0069.
 Skjoldan, P.F.: Aeroelastic modal dynamics of wind turbines including anisotropic effects. Ph.D. Thesis, DTU Risoe-PhD-66, 2011.

Comments to final revision:

Both references were adjusted as described above

Point 2: Details on the inflow characterization:

In order to evaluate if the samples used include sufficient atmosphere conditions, one must know the atmosphere conditions of the terrain and the terrain topology. More details are therefore needed for this:

Question 2:

p3L75: instead of giving the wind speed and turbulent intensity range (2m/s → 15 m/s Ti = 3% → 30%), please give the wind roses for the wind speed and the Turbulent intensity used in the study.

Question 3:

P3L73: "the cycles were performed during several months..."
 Please be more specific, how many months, which months?

Question 4: what is the type of sensor and their acquisition frequency?
 Can you evaluate the atmosphere stability with these sensors for instance?

Question 5:

Where are the 10 height measurements (including the topology of the terrain)?

Reply to question 2: A plot showing turbulence intensity as a function of wind speed for both measurement campaigns is included

Reply to question 3: This is specified in Table 1 (see below)

	Phase 1	Phase 2
Date	Oct 2017 - June 2018	Dec 2018 - June 2019
Turbine	SWT-4.0-130	SWT-4.0-130
AFS revision	FT008rev9	FT008rev10
AFS actuation	discrete positions	continuous angle variation
Actuation validation type	on-off cycles	on-off cycles
Location on blade	47.5 - 62.5 m	42.5 - 62.5 m

Table 1. Campaign information

Reply to question 4: The sensor signals of the met-mast are provided by an external supplier: in this case SGRE has a contract with the DTU dependency at the Høvsøre test center as responsible party for the calibration of meteorological instruments and signal availability. Due to this, the sensor manufacturer is not known. Nevertheless, it is the same type of instrumentation that at SGRE normally is used for power

performance measurements compliant with IEC61400-12 and the sensors are compliant with the norm requirements.

The acquisition frequency is 25Hz for the instruments in the metmast and 1Hz for the lidar signals, this is mentioned in page 3 line 65.

With regards to atmospheric stability, this is normally the case when no Lidar data is available, and the atmospheric stability is then estimated via the Monin-Obukhov length. In the current measurement setup, the direct profile is measured, and the additional information of the mixing length parameter for stability analysis is not relevant.

Reply to question 5: The measurement heights are (measured above ground): 38, 47, 59, 71, 83, 95, 107, 131, 143, and 155m

The site is flat (ie. It is flat in accordance to the requirements of table B.1 of annex B of IEC61400-12-1). A reference to a report on 10 year boundary layer meteorology at Høvsøre will be included in the paper.

If the terrain complies with the requirements of Table B.1, then no site calibration is required.

If the terrain characteristics are within an additional 50 % of the limits of the maximum slopes shown in Table B.1, then a flow model can be used to determine if a site calibration measurement can be avoided. The flow model shall be validated for the type of terrain. If the flow model shows a difference in wind speed between the anemometer position and the turbine's hub less than 1 % at 10 m/s for the measurement sectors, then no site calibration measurement is required.

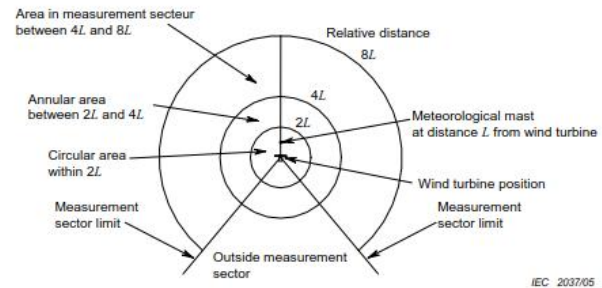
Otherwise a site calibration measurement is required.

Table B.1 – Test site requirements: topographical variations

Distance	Sector	Maximum slope %	Maximum terrain variation from plane
$< 2L$	360°	$< 3^\circ$	$< 0,04 (H+D)$
$\geq 2L$ and $< 4L$	Measurement sector	$< 5^\circ$	$< 0,08 (H+D)$
$\geq 2L$ and $< 4L$	Outside measurement sector	$< 10^{**}$	Not applicable
$\geq 4L$ and $< 8L$	Measurement sector	$< 10^\circ$	$< 0,13 (H+D)$

* The maximum slope of the plane, which provides the best fit to the sectoral terrain and passes through the tower base.

** The line of steepest slope that connects the tower base to individual terrain points within the sector.



Comments to final revision:

A small description of the site is given, but then a reference to the work of Peña et al. is given for further reference.

Point 3: Details on the actuator set-up

The description of the actuator system is never explicitly given. We don't know actually how the actuator is working unless we go to the publication from Gonzales et al (2028).

A Gomez Gonzalez, P B Enevoldsen, B Akay, T K Barlas, A Fischer, H Aa Madsen Experimental and numerical validation of active flap for wind turbine blades. Journal of Physics: Conf. Series 1037 (2018) 1234567890 “” 022039

This is particularly annoying to evaluate if the targeted objective (load control) is reachable. The needed time response of the system for load control (due to shadow effect) seems to be not reachable from the present system. Delays come from the whole control system arrangement itself, one order of magnitude slower. Indeed, this can't be the time response of aerodynamic loads which is faster, of the order of 0.2s (for 1.25m blade chord and a relative velocity of 60m/s). Moreover, this delay does not include the whole system:

P10L172: “The pressure response measurement of the transient analysis must be used with care due to the physical distance between the location of the actual measurement, and the location of the AFS. The pressure is measured directly at the exit supply valve.”

Question 6: A more detail description of the actuation system with the tubing arrangement (including the valve type, dynamic characteristics) should be included to at least evaluate what objective can be reached by this control system.

The general comments of point 3 require further clarification from our side. The purpose of the test was to do a technology demonstration at full-scale in order to start discovering the limitations of the systems and to perform a technology exploration. It was never the objective to test a particular controller strategy (this was also mentioned several times during the presentation at the conference). I will make this more clear in the paper.

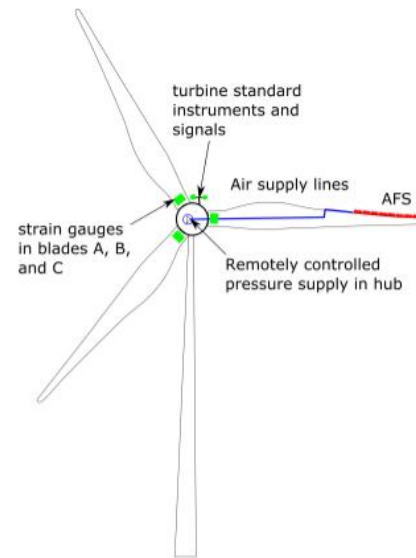
Therefore, the system is currently responding according to the physical limitations of the setup, including the pump capacity for air supply, as well as the gas dynamics of flow compression and viscous losses in the supply pipes (which are located inside the blade as the sketch below shows.

Therefore, we are not proposing that the current system is meant for load alleviation in its current state due to the time response. This also led to a very nice discussion during and after the conference presentation. Here I emphasized again, that the aim of the project was to design, install and test a technology demonstrator where we could be able to measure in full scale the available load handles, and further develop the methods required for measuring these with good accuracy (which was the blade-2-blade comparison method developed and described in the paper)

Reply to question 6: Yes, due to conciseness and page limitation, the reader is referred to the publication mentioned. All pneumatic components are placed in the hub. Air is supplied with a two pumps working in parallel of type Parker T1-2BL-24-1NEA. The valves used for control are in a 3/2 arrangement made up of 2 valves of type SMC VXZ24OFZ2AA 1/2", one in NC configuration and the second one in NO configuration. This will be mentioned in the paper.

Comments to final revision:

All amendments mentioned below have been included in section 2 – Test Description



Question 7: It seems that the control system is mostly interesting for power control. In that case, it

is important to evaluate the net benefit.
 Can you provide more details on at least the power supply needed to compress the air ?
 At maximum the impact of the additional weight and the impact on the rotor imbalance should be provided.

Reply to question 7: Similar as my reply to comments to point 3 above, the aim of the paper is not to demonstrate any control strategy, but to demonstrate a technology in full scale and measure the potential load impact. The system uses less than 0.5 kW at full operation pump speed, therefore, due to the low value, no further considerations to power consumption were made.

Rotor imbalance is not an issue. This demonstrator was installed with the AFS on a single blade with the purpose of subsequently being able to estimate the load potential with help of the blade-2-blade comparison method (which had not been possible with a full 3 blade installation). A real system would certainly have a 3 blade full blade installation, and therefore rotor imbalance would not play a role.

Comments to final revision:

	<p>A comment is made on the low power consumption of the system. No mention is done regarding rotor imbalance, as this is inherent to the b2b method described in the paper.</p>
<p>Point 4: Evaluation of the actuator impact:</p> <p>p6L95: “A standard method for this consist on the calibration of strain measurements in the root area of the blade, where strain gauges are placed on the intersection points between the contour of the blade and the principal axes of the section. With independent strain measurements of two different blades (and the corresponding transfer function to obtain bending moments), the integral load impact of an active device on a blade can be readily measured.”</p> <p>Question 8: The location of the strain gauges are not clear: which section is used ? Principal axis are not given. What transfer function are you using ? Are the bending moments known from another source ? What is the calibration procedure used in the present study ?</p> <p>Question 9: Also, the calibration of strain gauges on operating wind turbines is generally a long/heavy/costly and not accurate procedure. Is the evaluation of the bending moment necessary in the present blade to blade analysis ? Can't we use the strain gauge measure directly ?</p>	<p>Reply to Questions 8 & 9</p> <p>The strain gauges are located at 1.2m from the blade root at the intersections of the principal axis of that section with the blade contour. The geometrical information of the blade contour is SGRE proprietary and can therefore not be disclosed. It will be made a mention in the paper regarding the spanwise location of the strain gauges.</p> <p>The calibration procedure of strain gauges in the blades is quite straight forward and is performed for each one and every prototype turbine. These procedures are well known in the industry and some suggestions are also given in IEC 61400-13 (see screenshot below). For the present case, the calibration is performed is gravity based as described in section 4.2.2.2 of the standard aforementioned.</p>

4.2.2 Measurement of blade root bending moments

4.2.2.1 Instrumentation

Flap and lead-lag bending moments shall be measured. For lightning and environmental protection, it is recommended that the sensors be mounted within the blades rather than on the outer surface, where convenient. This will also lead to better protection during handling.

Strain gauges should be applied in such a position that cross-sensitivities between lead-lag and flap-load measurements are minimized. Applying the gauges to a part of the blade root which is as nearly cylindrical as possible may facilitate this. Regardless of the mounting location, cross-sensitivity should be measured and corrected according to B.2.1.

In the case of pitch-regulated turbines, the above advice also applies. However, for consistency, the sets of gauges should be oriented so that they are parallel to and perpendicular to the chord line at 70 % radius.

4.2.2.2 Calibration

The blade-root load sensors should be calibrated by external force application close to the blade tip. Alternatively, the signals for the lead-lag and flap-bending moment in the blade root can be calibrated using the blade mass as a calibration load in case the blade can be pitched over at least 90°. Since the load signals are designed to measure the bending moments in the blade root at the position of the strain gauges, the calibration has to be performed using the values of the mass and centre of gravity of the part of the blade outside the strain-gauge position for the determination of the calibration load. This requires exact knowledge of the distribution of the blade mass per unit length along the blade axis.

It should be noted that using the blade mass to calibrate the loads might limit the calibration load range and result in a higher calibration uncertainty.

4.2.2.3 Calibration check

By rotating the rotor slowly around 360°, the blade mass causes a variation in the lead-lag signal. If pitching is possible, the variation in the flap wise signal can also be measured. The variations have to be measured at initial calibration in order to determine the reference for repeated checks later on. This check shall be done at low wind speeds. When checking the lead-lag moments, it is recommended to yaw the wind turbine 90° in relation to the wind direction.

Comments to final revision:

Section 2 has been ammended to specify the placement of the strain gauges.

PGL104: "Furthermore, the uncertainty related to point-wise wind speed measurements is removed."

Yes, but this is valid only if the statistical converge is reached. Regarding the atmosphere changes, there is diurnal changes, seasonal changes, dependence on the terrain etc ...

Question 10: You should moderate this sentence, the uncertainty related to point-wise wind speed measurements is only smoothed and valid for a limited range in the atmosphere/terrain conditions (which are not given in the paper).

Reply to comment and to question 10: The blade-2-blade comparison method precisely addresses the diurnal and seasonal changes that you mention, because the AFS-blade and the other two reference blades are seeing the same inflow during the same 10-min interval, that is the nice thing about the analysis. It is analogue to side-by-side analysis of turbine performance when performed according to IEC. I will include this in the paper

Comments to final revision:

A comment to this has been done in section 3.1. The word "removed" is left in the text, as it really removed. This is because the analysis is based on load to load comparisons, and the wind speed does not play a role for this.

Question 11: There is certainly limitations that are linked to the statistical convergence of data, which is certainly dependent on the coherence of the turbulent wind field contrary to what is said in the text. In other terms, why 30 min and not 1hour, 2hours, 1 day ... for your statistics ? Have you looked on how the statistics converge towards the final value ?

Reply to question 11: For standard power and load measurements, intervals of 10 minutes are used as this normally covers the turbulence power spectrum of small scale atmospheric turbulence (see Van der Hoven spectrum below). 1 day is not chosen because you would have a clear day-night cycle in the data set. 1 hour or 2 hours could have also been options. We intended to gather a higher number of transients, therefore we chose 30 minutes instead of periods of 1 or 2 hours. We chose 30 minutes, and not 10 minutes (which else would have been standard), in order to avoid having a significant impact of the transient behavior on the steady state values. I will comment this in the paper.

Comments to final revision:

Section 2 has been ammended to include this comment

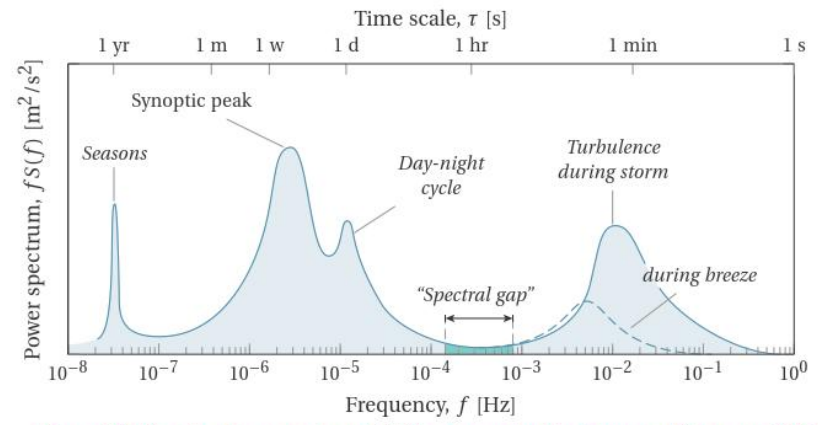


Figure 2.2: Van der Hoven spectrum (1957) as drawn by Alan Davenport (Isyumov, 2012).

Field test of an active flap system on a full scale wind turbine

Alejandro Gomez Gonzalez¹, Peder B. Enevoldsen¹, Athanasios Barlas², and Helge A. Madsen²

¹Siemens Gamesa Renewable Energy A/S, Brande, DK

²Technical University of Denmark DTU, Dept. of Wind Energy, Roskilde, DK

Correspondence: A Gomez (alejandro.gonzalez@siemensgamesa.com)

Abstract.

This article describes a series of validation tests of an active flap system (AFS) on a multi-MW wind turbine. A single blade of a 4 MW turbine with 130m rotor diameter (SWT-4.0-130) is retrofitted in the outer 15-20 m with the AFS. The AFS is controlled remotely with a pneumatic pressure supply system located in the hub of the turbine. The measurements are performed between October 2017 and June 2019 using two different AFS configurations on the blade. A description of the system setup is given, as well as comparisons of measurements and aeroelastic simulations. The measurements quantify the static load control authority of the AFS in atmospheric conditions, providing a preliminary estimate of load impact potential for the concept. The article presents furthermore a new method for the characterization of the load impact of such a system and its dynamic response under atmospheric conditions based on a blade-to-blade load comparison.

10 1 Introduction

Load control and performance optimization of wind turbines using active flap systems has been the subject of numerous studies in the past. It is not within the scope of this paper to give a comprehensive review of the state of the art of active flow control on wind turbines, but to focus solely on the efforts towards active flow control validation at full scale. For an extensive review of the state of the art in smart rotor control, the reader is referred to Barlas (2009), who covers both active control surfaces such as flaps and microtabs, but also other active flow control technologies such as boundary layer control or active twist. Furthermore, the reader is also referred to Pechlivanoglou (2013), who in his dissertation gives a broad overview of different active and passive control technologies for wind turbines as well as comparisons among them, as well as to Johnson (2008) also providing an overview of active load control strategies for wind turbines. Furthermore, a recent technical expert meeting of IEA Task 11 (TEM87, 2017) collects contributions from several groups within the field of active flow control including a variety of technologies such as active flaps (Riemenschneider, 2017; Berg, 2017; Enevoldsen, 2017), plasma actuators (Pereira, 2017), and active leading edges (Holling, 2017), among others.

At wind tunnel scale, Pechlivanoglou (2017) and Samara (2018, 2020) demonstrate the use of active trailing edge flaps on a 3m and 3.5m diameter model wind turbine model at the TU Berlin and the University of Waterloo, respectively. Samara (2020) investigates the control authority of the flap system benchmarking it to the pitch system of the turbine. In these tests, an active flap segment of 20% chord and 22% span coverage was installed on the wind tunnel model. The tests performed reveal that a

flap angle actuation in the range from -20 to +20 deg is similar in terms of load impact to a full section span pitch actuation in the range from 0 to 9 deg.

In terms of full scale validation of active flow control on wind turbines, the academic and industrial contributions are scarce. In the decades prior to the modern boom of wind energy, active flow control on wind turbine blades seemed almost natural, as the technology used for the development of turbine blades was driven mainly by know-how transfer from the aeronautical industry. A clear example of this is the design of a 7.3 MW, 122m rotor diameter turbine within the frame of the MOD-5A program in the early 1980's (MOD5A, 1984). In the design of this turbine, which was never commercialized, three independent ailerons, fully integrated in the outboard section of the blades and activated with a hydraulic system, were used both for loads and power control. Nevertheless, the active flow control strategy of the MOD-5A turbine was not the focus at that time, but rather a choice taken at one of the later design stages as it was believed that this control strategy would be more economically viable than the alternative considered: partial pitch control of the blade. The ailerons were designed as plain hinged flaps extending from approx 60% to 99% of the chord.

In more recent years, a series of tests were performed by RISØ Laboratories in collaboration with Vestas Wind Systems A/S on a Vestas V27-225 kW turbine (13m blade length) equipped with a 70 cm long trailing edge flap as described by Castaignet (2010, 2013a). During the test, which spanned for several hours split among several days, the turbine load control with active flaps was ran in intervals of 2 minutes with, and 2 minutes without the flaps active. During 10 of these measurement intervals, an average blade root flapwise fatigue load reduction of 14% was achieved for a test running 38 minutes using a frequency weighted model predictive control. The controller strategy for this test is further discussed by Castaignet (2013b) and Couchman (2014).

A further full scale test of an active flap system is given described by Berg (2014a, b), where the 9m long CX-100 blade was retrofitted with active flaps integrated in the structure. For this purpose, a rigid hinged flap was incorporated in the trailing edge area of the original blade. The effective hinge area of the flap covered the aft 20% of the chord, of the outboard 20% of the blade span (approx. 2m of the blade). The flap was actuated with a motor embedded in the structure both in constant offsets as well as sinusoidal actuation. During these tests, a significant loss of power production was measured, which is thought to have a relation either to a lack of stiffness of the active flap, an error in blade pitch, or aerodynamic losses due to changes of the aerodynamic performance of the airfoils. The tests also served the dynamic characterization of the system in terms of frequency response and the transient characteristics in terms of time delays.

One relevant (non-flap) active flow control full scale test performed on a 1.75 MW wind turbine is described by Matsuda (2017). This test focuses on the use of plasma actuators installed on the leading edge of the blades with the purpose of flow separation control. The tests were performed in swap intervals of 10 minutes and focusing on the effect on the turbine's power production. When the plasma is turned on, a rotor speed increase was measured. For a test period of 22 h distributed over 6 days, an average power increase of 4.9% was measured.

Within the framework of the recent EU project INNWind, an active morphing trailing edge was tested under atmospheric conditions at the Risø campus of the Technical University of Denmark on an outdoor rotating test rig (Ai, 2019; Innwind2.3.3, 2017; Barlas, 2018). The tests conducted herein included both step flap actuation, as well as feed-forward control based on

periodic azimuth variations and also inflow measurements. In contrast to the 2 min cycles of the tests described by Castaignet (2010), these swap tests were performed in 10s cycles over a test period of 5 minutes, repeating this procedure for different operation conditions. The results of these tests showed lift coefficient variation levels in the range of -0.25 to +0.2 (for the step flap tests). Feed forward control tests based on azimuth position and inflow angle showed a reduction of the standard deviations of the flapwise bending moment at the base of the boom of the rotating arm of the rig of 12% and 11%, respectively. In similar tests on the above mentioned rotating test rig described by Madsen (2015a) within the framework of the Induflap1 project, an active flap with 15% chord coverage was tested in flap angle activation steps. A flap angular step magnitude of 5 deg was estimated to be equivalent to a 1 deg full section pitch actuation, similar to the results of Samara (2020).

A good example of the study of active flaps as a potential technology for reduction of LCOE is given in deliverables 2.23 and 2.33 of the InnWind project - see final report Innwind (2017). A significant reduction in blade flapwise fatigue loading is obtained by a combination of individual flap control together with individual pitch control.

The work described in the context of this paper consists of a full-scale long-term validation of two different revisions of an active flap system (described in the next section) on a SWT-4.0-130 turbine. A numerical and experimental characterization of the first revision of the active flap component can be found in (Gomez, 2018). The main purpose of the test is to make an overall aerodynamic and load-wise performance characterization of the system and not to test any specific closed-loop control strategy. Furthermore, the tests presented herein were performed with the goal of characterizing an innovative solution, which in contrast to what has been done in the past, is tested in industrial full scale, during a long period, with remote control and surveillance, as well as with high quality data acquisition of both the turbine and inflow data.

2 Test description

The test setup consists of a SWT-4.0-130 turbine (63.4m blade length) retrofitted with the Active Flap System (AFS) on one of the blades, located at the test site Høvsøre, 2 km from the west coast of Denmark. The site is characterized by flat terrain and normally low turbulent flow with a predominant west wind direction. A thorough description of the atmospheric characteristics of the site is given by Peña (2015). The turbine was equipped with a pressure supply system with two pumps working in parallel of type Parker T1-2BL-24-1NEA for the pneumatic activation of the AFS. The air flow was controlled with supply valves in a 3/2 arrangement made up of 2 valves of type SMC VXZ24OFZ2AA 1/2G, one in NC configuration and the second one in NO configuration. Both the pumps and the valves were located in the hub of the turbine. From here, the air was supplied to the AFS via hoses running both along the inside and the outside of the blade up to the start location of the AFS. An internal inflatable hose was responsible for the hinge actuation mechanism at the trailing edge of the airfoil where the AFS was installed. The total power consumption of the system is below 0.5 kW. All systems were designed to be activated remotely interfacing through the turbine communication unit. Two versions of the AFS were tested in independent campaigns as shown in figure 1. The two flap revisions used in phases 1 and 2 are referred to as FT008rev9 and FT008rev10, respectively. Test phase 2 was improved taking into account learnings from phase 1. During phase 2 of testing, besides upgrading the AFS to a newer, more aerodynamically and structural optimized geometry, an upgrade of the pressure supply system was performed focusing on increasing the air

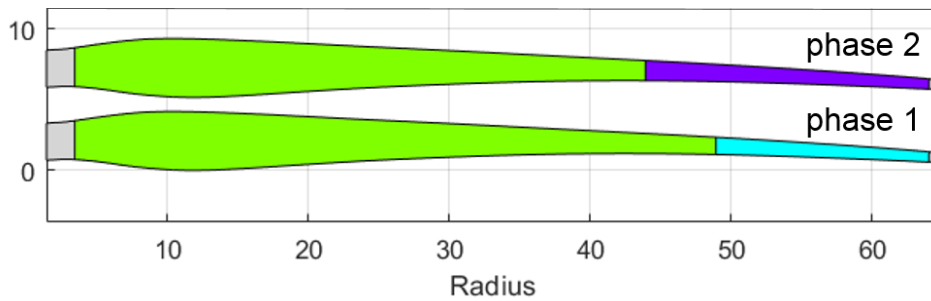


Figure 1. Blade layout of AFS

	Phase 1	Phase 2
Date	Oct 2017 - June 2018	Dec 2018 - June 2019
Turbine	SWT-4.0-130	SWT-4.0-130
AFS revision	FT008rev9	FT008rev10
AFS actuation	discrete positions	continuous angle variation
Actuation validation type	on-off cycles	on-off cycles
Location on blade	47.5 - 62.5 m	42.5 - 62.5 m

Table 1. Campaign information

storage capacity of the system, as well as a new system allowing continuous variation of pressure levels (in contrast to phase 1, where only discrete levels are used) - see table 1 for reference. Therefore, the tests presented herein will focus mainly on test phase 2.

The system installed in the turbine meets the requirements for an accurate measurement of the load handle available by the use of a particular type of active flap, but has technical limitations for the implementation of high frequency closed-loop control (e.g. pump capacity, transients related to gas expansion, and viscous losses). Therefore, the tests presented herein are meant as a technology demonstration, and not as a demonstration of a specific control strategy.

For the validation of the load impact of the AFS, the turbine was instrumented with strain gauges at a distance of 1.2m from the root of all three blades (configured to measure flapwise and edgewise bending moments) as well as at the tower top position. Per default, all operational parameters of the turbine such as pitch, rotor speed, and power are continuously logged. The wind speed and direction, as well as atmospheric pressure, temperature, and humidity, are measured on a met-mast located 2.5D in front of the turbine. The wind speed and direction at 10 different heights throughout the full extension of the rotor (distributed between heights of 38m and 155m above ground level) are measured with a nearby Lidar in order to have a good assessment of shear and veer (see figure 2). The pressure level of the AFS, as well as the digital signals for activation of supply valves are logged synchronously with all other quantities. The pressure-deflection characteristic of the flap is known from previous wind tunnel measurements (Gomez, 2018). All quantities are logged continuously for the full measurement period with a sampling



Figure 2. Test site layout. Map data taken from GoogleMaps copyright - 2020

110 frequency of 25 Hz (except the lidar signals, which are sampled with 1 Hz). In addition, the blade is equipped with a remote surveillance camera in order to monitor the AFS (see exemplary view in figure 3 and 4).

The primary characterization of the system is performed by actuating the flaps using pressure steps (equivalent to steps of flap deflection angles), cycling through different pressure levels over constant time intervals. Contrary to the work of Berg (2014a), where the cycles chosen were of 30s, or the work of Castagnet (2013a) with 2 minute cycles, the cycles chosen for
 115 the current work are 30 minutes long, allowing both to gather the high frequency transient response of the system, as well as three independent 10-min time stamps of statistical power and load values for every cycle. For standard power and load measurements, the averaging interval of a single measurement point is 10 minutes as this normally covers the turbulence power spectrum of small scale atmospheric turbulence. An interval of 30 minutes captures three sequential measurement values, and allows the system to shift to a different operation condition such that during a full measurement day, the turbine together with
 120 the AFS system will be operating numerous times in different modes, avoiding thus that any day-night variations can have an effect on the load comparison.

The cycles were performed during several months, cycling through different flap deflection levels, allowing therefore data acquisition over a very wide range of wind and operating conditions. During the measurement periods, the AFS operated at wind speeds covering the range of approx. $2 \frac{m}{s}$ to $15 \frac{m}{s}$ for turbulence intensities between approx 3% and 30% as shown in
 125 figure 5.

The aerodynamic characteristics of the AFS operated at different pressure levels are known from previous wind tunnel measurements as described by Gomez (2018). An example of the measured normalized aerodynamic coefficients for the first revision of the AFS (FT008rev9) is shown in figure 6 (depicting the impact on lift coefficient and gliding ratio of the airfoil). The curve labeled as *baseline* represents the airfoil without AFS.



Figure 3. Active flap seen from hub



Figure 4. View of flap activation

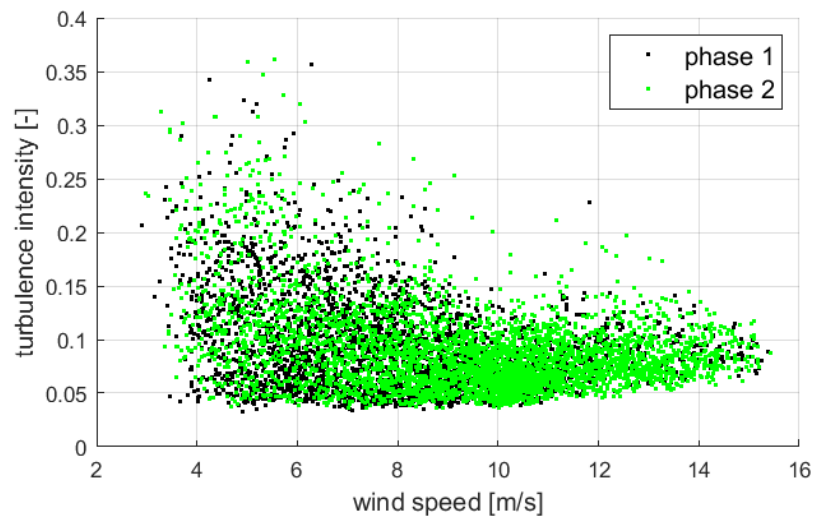


Figure 5. Turbulence intensity as a function of wind speed for phase 1 and 2 of the measurement campaign

130 3 Results

This chapter gives a summary of results obtained for both field test campaigns of the AFS. For both campaigns, a series of activation tests were performed to ensure the correct functionality of the system. Visual checks were also performed in order to verify the flap is deflecting properly and is not blocked or restrained in any way.

Due to the stochastic nature of the measurements (with varying levels of inflow turbulence, shear, etc.), the comparison of
 135 loads as a function of wind speed is not the best choice. Measured variables as a function of wind speed normally have high scatter due to atmospheric variability, but also due to the coherence effects between the measurement point of the undisturbed wind speed (the met mast), and the location of the turbine. Due to this, a new method for analysis is developed, consisting of a blade-to-blade load variation representation. For this purpose, neighbouring blades are used for the analysis based on flapwise

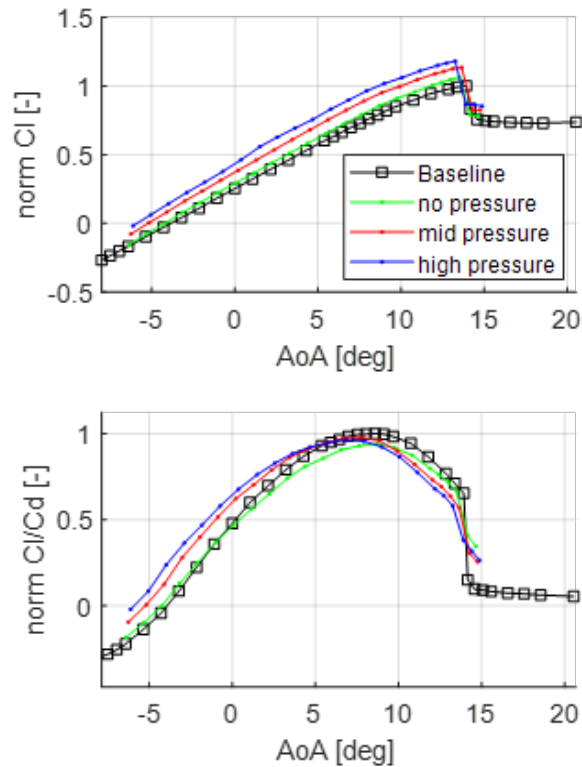


Figure 6. Exemplary normalized aerodynamic coefficients for FT008-rev9 AFS

bending moment measurements via strain gauges placed at the root of the blades. Utilizing this method, the uncertainty related
 140 to inflow conditions as well as to coherence in the wind field is removed to a large extent. In what follows, a description of the
 method is given.

3.1 Blade to blade analysis

The blade-to-blade analysis method (referred to as b2b-method in what follows) consists mainly of two independent types of
 analysis: a **steady state**, and a transient analysis.

145 The **steady state analysis** is quite straight forward and requires only a turbine equipped with a calibrated means of measuring
 bending moments. A standard method for this consists on the calibration of strain measurements in the root area of the blade,
 where strain gauges are placed on the intersection points between the contour of the blade and the principal axes of the section.
 With independent strain measurements of two different blades (and the corresponding transfer function to obtain bending
 moments), the integral load impact of an active device on a blade can be readily measured. One of the blades of the turbine is
 150 equipped with the active device in question, whilst the other two blades are left unchanged. In this fashion, the two unchanged

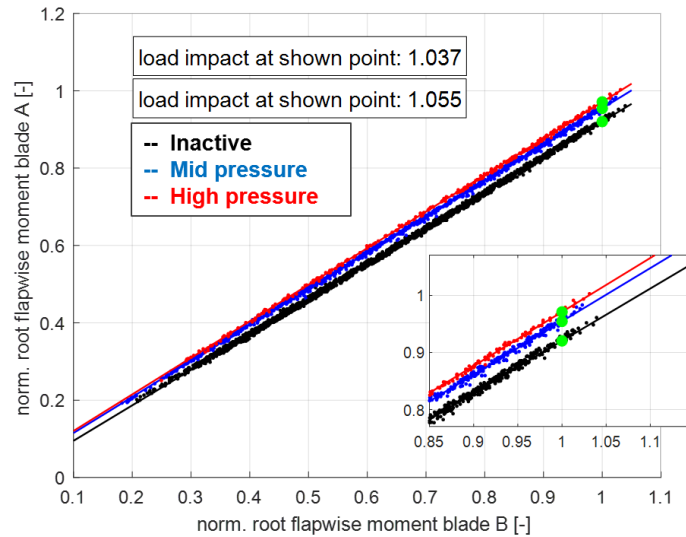


Figure 7. Example of a time averaged blade to blade load comparison

blades serve as reference for comparison. This type of comparison between the blade retrofitted with the AFS and the baseline blades has quite low scatter, as both blades are seeing all the time the same time averaged impact of shear, turbulence, veer, and turbine dynamics. Avoiding the use of wind speed measurements increases greatly the correlation of the measured signals because there is no dependence on the coherence of the turbulent wind field. Furthermore, the uncertainty related to single-
 155 point wind speed measurements (e.g. related to single point measurements at the met mast for power performance estimation) is removed because the comparison is being done between two load quantities directly, which in their nature are integral quantities (similar to the high correlation which exists between the power signals of two neighbour turbines). A similar method has been previously used by Bak (2016) to evaluate the impact of vortex generators on a full scale wind turbine. An example of such b2b comparison between the blade equipped with the AFS and a reference blade is shown in figure 7, where normalized
 160 flapwise bending moments are shown for blades A and B for three different pressure levels for the AFS.

The purpose of the *transient analysis* part of the b2b-method is to extract the transient response (in this case, the step response) of the system as it undergoes changes in time. The complexity of measuring the transient aerodynamic response lies in the fact that this type of high frequency response will normally be hidden in the dynamics of the blades responding to turbulence, vibrations, rotation, etc. The core of the transient analysis of the b2b-method relies on the elimination of the
 165 periodic signal dynamics due to rotation and forced vibrations via an artificial time-shift of signals of neighboring blades, together with the elimination of the dynamics due to turbulence via time filtering and ensemble averaging.

The *first step* of the transient b2b-method is to read the bending moment signals from all three blades (the blade retrofitted with the AFS, and the remaining two blades as reference) a sufficient amount of time before and after the dynamic change of the system (e.g. a pressure step of the AFS). Such signals are shown exemplary in figure 8b.

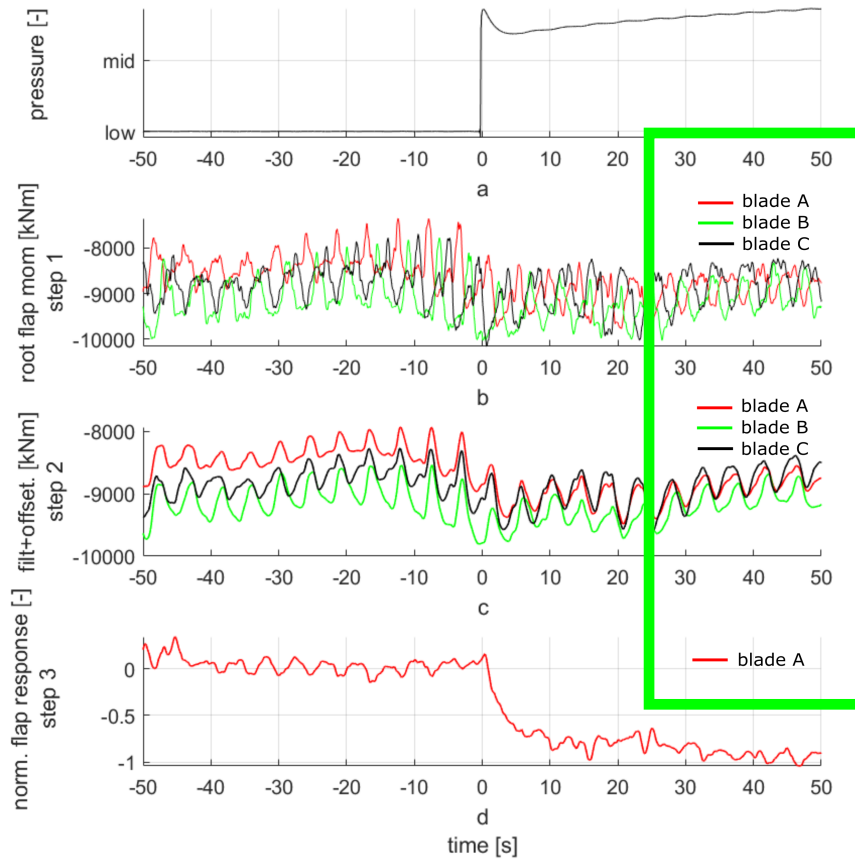


Figure 8. Transient signal analysis

170 The *second step* consists on a low-pass filtering of all signals with an appropriate time constant and a subsequent time shift. In the current analysis, all signals were filtered using a low-pass first order filter with a $1s$ time constant (see figure 8b). The time constant must not be too large, else it has an impact on the dynamics due to the natural phase-shift effect of the filter, and should not be too small else there will be a large amount of high frequency cycles which will still be visible after the ensemble averaging. The leading and trailing baseline blades are shifted backwards and forward in time, respectively, by $\Delta t = \pm \frac{2\pi}{3\bar{\Omega}}$,
 175 where $\bar{\Omega}$ is the average rotor speed expressed in rad/s during the respective period. The output of this step is shown exemplary in figure 8c, where in contrast to figure 8b, the signals are now clean of high frequency content and have peaks aligned in time.

The *third step* of the method is to detect the point in time where the dynamic change of the system takes place, and to time-shift the signals such that this time corresponds with $t = 0$ (see example in figure 8a). This will be important for the next step (the ensemble averaging). For the current work, the controller actuation signal of the supply valve of the system

180 was read directly, knowing then precisely the starting time of the transient response. At this stage, the bending moments of both reference blades are averaged. This average reference value is then subtracted from the bending moment signal of the blade equipped with AFS, and this differential load is normalized based on the amplitude of the load step, leading thus to the normalized impact on loading from this single blade. An example of the result of this stage of the signal processing is shown in figure 8d.

185 The *fourth and last step* of the transient response extraction is the ensemble averaging of these delta loads across several actuations, such that the stochastic variations are averaged out (e.g. variations due to turbulence). This is shown in the results section in figures 13 and 14.

3.2 Field measurements

The first section of results relates to the steady load impact of the AFS used in phase 1 and phase 2 of the field test. The relation
190 between the flapwise blade root bending moment and wind speed is not monotonic. For modern pitch controlled turbines, the flapwise moment will increase with wind speed until it reaches a maximum close to the region of rated power and in this region the angle of attack (AoA) variations as a function of wind speed are small. Subsequently, the flapwise bending moment will decrease as wind speed further increases, and the AoA of the blade sections will decrease as the blade pitches into the wind. Due to this non-monotonic behaviour of the bending moment and the related changes in AoA, it is important to differentiate
195 between regions of low and high wind when doing the time averaged analysis. For the measurements referred to here, the data sets were divided into measurement points with 10-min average wind speed below and above $9 \frac{m}{s}$, respectively.

All 10-min bins during the measurement periods of phase 1 and 2 were collected and split into low and high wind areas. For this data set, the b2b comparison between blade A (equipped with the AFS) and blade B (one of the baseline blades) is shown in figures 9 through 12. There is a high correlation between these bending moment measurements (seen by the linear relation
200 and the very low scatter of the plot). Furthermore, the data is filtered based on two different pressure levels representing the operation envelope of the active flap system. The impact of the active system is seen in the fact that two clearly defined lines are seen in these plots. The relative change of loading of blade A vs. blade B at different locations along these lines represents the impact of loading measured at the blade root for different wind speeds. The load levels have been normalized for clarity, where the normalization factor has been chosen as the average peak loading of the bending moment vs. wind speed curve. Therefore,
205 values close to 1 in these figures represent peak loading of the turbine and are representative of the maximum loading level of the turbine (corresponding to wind speeds close to $9 \frac{m}{s}$). For very high operational wind speeds (for example $15 \frac{m}{s}$ and above), the bending moment will decrease as already discussed. For this wind speed range, a representative normalized load value of 0.66 is chosen. These two values (1 and 0.66), representative of peak loading and high wind speed loading, respectively, can be seen highlighted in figure 9 through 12 together with the corresponding load ratio.

210 It can be seen that for phase 1, the load impact at the blade root is measured to be in the range between 3% and 4.2%, whereas for the phase 2, the loading ratio increases up to approx. 5.6% to 10%. It is worth mentioning that the load ratios for outboard locations of the blade which are closer to the AFS will be larger, but these values were not measured during this field

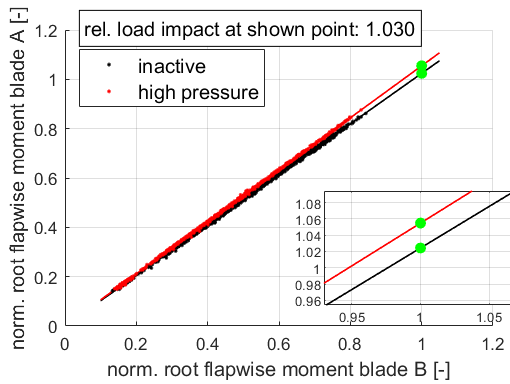


Figure 9. Test phase 1, $ws < 9 \frac{m}{s}$

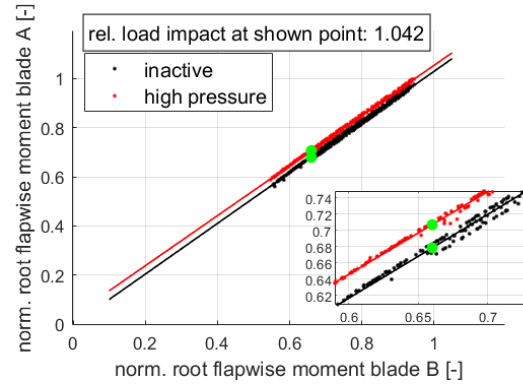


Figure 10. Test phase 1, $ws > 9 \frac{m}{s}$

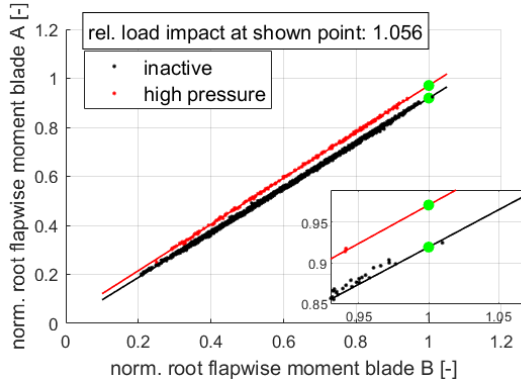


Figure 11. Test phase 2, $ws < 9 \frac{m}{s}$

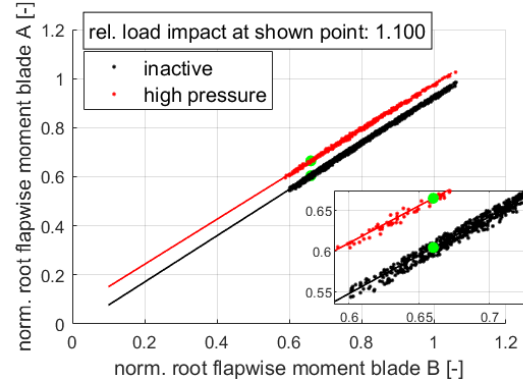


Figure 12. Test phase 2, $ws > 9 \frac{m}{s}$

test. The load handle of 5% to 10% obtained in phase 2 is one of the major results of the project, highlighting the potential of the AFS to manipulate actively the loads of the turbine.

215 For the transient analysis of the data accumulated during the field test, the different changes in pressure of the AFS were categorized depending on the start and end value of the pressure level. The data presented herein is given for so-called type H1 and type L2 pressure steps. Type H1 represents a step change in pressure from the lowest to the highest threshold of the system, whereas a type L2 step represents a step change from the highest towards the lowest pressure thresholds. This means in other words that type H1 represent a full activation of the AFS, and type L2 the deactivation. These two type of pressure jumps show different dynamic behavior due to the differences in flow dynamics during the inflation and deflation of the AFS. 220 The ensemble averaged response of the H1 and L2 pressure steps are depicted in figures 13 and 14. For the analysis shown, the number of individual time series analyzed is given in the plot with the value N. Every dynamic step is extracted at the end / beginning of one of the 30 minute intervals described earlier.

The pressure response measurement of the transient analysis must be used with care due to the physical distance between 225 the location of the actual measurement, and the location of the AFS. The pressure is measured directly at the exit supply valve.

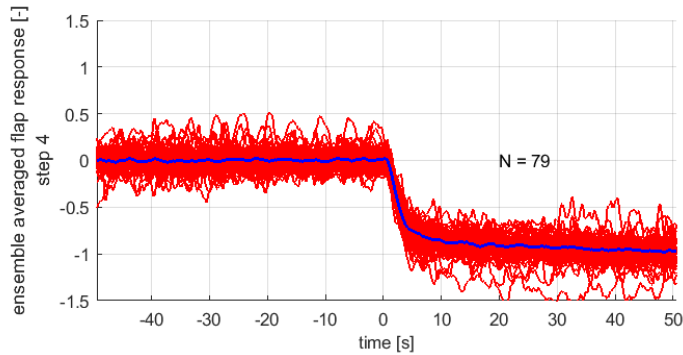


Figure 13. Pressure step type H1

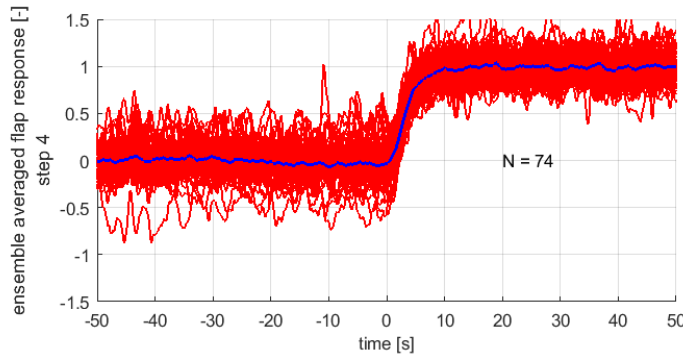


Figure 14. Pressure step type L2

This pressure signal is used for filtering the measurements according to the pressure level, but not for the dynamic analysis as it does not represent accurately the instantaneous pressure at the AFS location (due to the flow dynamics in the pressure supply line). The pressure level at the location of the AFS was not measured in these test campaigns due to the long-term duration of the measurements to avoid interference with the lightning protection system. Nevertheless, with the pressure transient at the supply valve location during the activation sequence, it can be seen that the air supply to the AFS reaches saturation (this can be seen from the slow increase in pressure) and will be addressed in future developments.

3.3 Aeroelastic simulations

Aeroelastic simulations are performed with SiemensGamesa's in-house solver BHawC see Rubak (2005) and Skjoldan (2011). The simulations are performed in a so-called one-to-one fashion (o2o) (see Enevoldsen (2018) for reference). The o2o calculations are high fidelity aeroelastic simulations performed in a *digital twin* manner, meaning that the structural model is matched exactly to the particular turbine under consideration both in geometry, structural description, and system dynamics, but also where every single 10 min atmospheric inflow measurement point is recreated numerically. The aerodynamic input to the simulation in form of airfoil polars is taken directly from wind tunnel measurements of the AFS. For the full period of phase 1

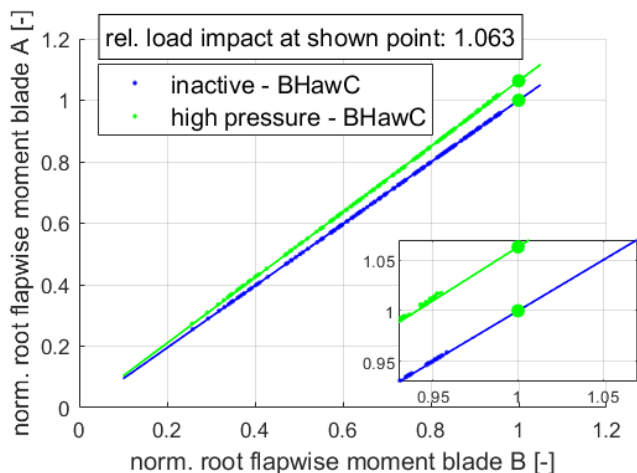


Figure 15. Phase 2 simulations at low wind

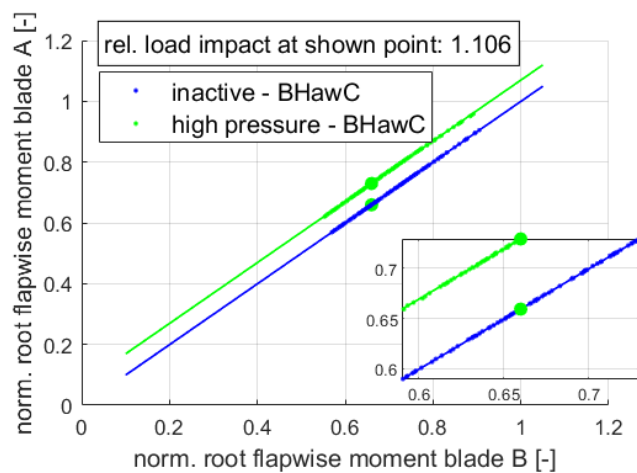


Figure 16. Phase 2 simulations at high wind

and phase 2 of the field test there exists therefore the same corresponding period of o2o equivalent aeroelastic simulations. The input to the simulations is dependent on good inflow measurements and therefore only the wind sector where the metmast / lidar is unaffected by the wake of any turbine of the park is used for comparison. For this reason, even though the b2b method is generic for the whole range of directions, only the west sector is taken in consideration for o2o simulations ($270 \pm 30deg$).

The simulations results presented here focus on phase 2 of the measurement with AFS FT008rev10. In figures 15 and 16, the time-averaged b2b simulation results for the blade equipped with AFS and a baseline blade are shown. These results, similarly as for the experimental results, are shown for low wind and high wind regimes below and above $9 \frac{m}{s}$, respectively. As can be seen from the figure, the aeroelastic simulations are in very good agreement with measurements, predicting a load impact of 6.3% representative for peak loading, compared to the measured 5.6%, and 10.6% compared to the measured 10.0% representative for high wind situations (cp. figures 10 and 12).

3.4 Discussion of results

Both the aeroelastic simulations as well as the full scale validation of this flap concept show a load handle which allows to actively adjust the blade root flapwise loading level in the range of 5%-10% depending on the wind speed range. This load handle comes at the cost of a slight reduction in gliding ratio (see figure 6). Even though a reduction of gliding ratio would normally be related to a loss of aerodynamic performance, this is only true for "non-active" blades, and affects mainly the variable speed region of turbine operation. The reason for this is that the aerodynamic performance is also influenced by the induction levels of the blade, which in turn are highly dependent on the lift level of the airfoils. Depending on the general induction level of the rotor, the blade design strategy (in terms of induction spanwise distribution), and the operation characteristics in the constant speed area just before rated power, the power performance of a modern turbine will usually be more sensitive to variations of lift levels, than to changes of gliding ratios. In this area of the power curve, the ability to

increase lift levels will in general overshadow small penalties of gliding ratios. Following this line of thought, an offshore turbine operating at a site with high mean wind speed and having a wide constant speed region prior to rated power, will be less sensitive to gliding ratio penalties and will benefit more from the ability to actively change lift levels, than a smaller onshore turbine at a low wind speed site with a wide variable speed range.

A potential load handle of 5-10% is certainly interesting from a wind turbine design perspective. Such a load handle can be used in two ways: the first one is during the design phase of a new platform in order to enable a more cost effective dimensioning of the main components, and the second one is to upscale the rotor of an existing platform while maintaining the loads within the allowable envelope, having thus a positive impact on LCOE - see e.g. Barlas (2016).

4 Conclusions

Two independent long term validation campaigns were conducted for a pneumatic active flap system on a full scale wind turbine. The AFS was actuated in an on-off fashion in order to assess the load impact of the system. The first revision of the AFS was activated at discretely varying pressure levels and showed a potential load impact between 3-4% for root flapwise bending moments. In a second phase of the testing campaign, the AFS was optimized both aerodynamically and structurally, in combination with an upgrade of the pressure supply system which enabled continuously varying angle activation. This revision of the AFS showed a potential load impact between 5-10% at the root of the blade.

The measurements performed were accompanied with high fidelity aeroelastic simulations where the aerodynamic input was based on polars measured in a wind tunnel, and the atmospheric inflow was based on metmast and lidar measurements. Very good agreement was found between the measurements and the simulation results.

The AFS was shown to operate in a robust way and without major drawbacks. The AFS revisions were tested independently for over 6 months each, covering therefore a wide range of wind speeds, temperatures, and atmospheric conditions. The loads of the turbine were measured as well in a robust and accurate manner, enabling a good estimate of the potential load impact levels of the AFS. Finally, a novel method was developed in order to directly measure the transient behaviour of the AFS in a highly time varying environment.

Author contributions. All authors contributed significantly to the work presented within this paper.

Competing interests. The authors declare they have no competing interests.

Acknowledgements. The work presented in this article is part of the Induflap2 project (Induflap2) which is a research and development project carried out in the period from 2015 to 2019. The authors wish to acknowledge EUDP for the funding given to the project (journal nr. 64015-0069).

References

- Ai, Q., Weaver, P.M., Barlas, T.K., Olsen, A.S., Madsen, H.Aa., and Andersen, T.L.: 2019 Field testing of morphing flaps on a wind turbine blade using an outdoor rotating rig, *Renewable Energy*, vol. 133 pp. 53-65, 2019.
- 290 Bak, C., Skrzypinski, W., Gaunaa, M., Villanueva, H., Brønnum, N.F., and Kruse, E.K.: Full scale wind turbine test of vortex generators mounted on the entire blade, *J. Phys.: Conf. Ser.*, 753-022001, 2016.
- Barlas, T.K. and van Kuik, G.A.M: Review of state of the art in smart rotor control research for wind turbines *Progress in Aerospace Sciences*, vol. 46, 1–27, 2010.
- Barlas, T.K., Pettas, V., Gertz, D., Madsen, H.A.: Extreme load alleviation using industrial implementation of active trailing edge flaps in a full design load basis, *The Science of Making Torque from Wind TORQUE2016*, *J. of Phys. Conf. Series*, vol. 753, 2016.
- 295 Barlas, T.K., Olsen, A.S., Madsen, H.A., Andersen, T.L., Ai, Q. and Weaver, P.M.: Aerodynamic and load control performance testing of a morphing trailing edge flap system on an outdoor rotating test rig, *Journal of Physics: Conference Series*, vol 1037(2), 022018 <https://doi.org/10.1088/1742-6596/1037/2/022018>, 2018.
- Berg, J., Resor, B.R., Paquette, J.A., and White, J.: SMART wind turbine rotor: design and field test, Sandia National Laboratories, Wind Energy Technologies Department, SAND2014-0681, Albuquerque, USA, 2014.
- 300 Berg, J., 2014, Barone, M.F., and Yoder, N.C.: SMART wind turbine rotor: data analysis and conclusions Sandia National Laboratories, Wind Energy Technologies Department, SAND2014-0712, Albuquerque, USA, 2014.
- Berg J.: Smart Rotor Project Summary, Proceedings of the TEM87 Smart Blades Expert Meeting IEA Task 11, Copenhagen, 2017.
- Castaignet, D., Barlas, T.K., Buhl, T., Poulsen, N.K., Wedel-Heinen, J.J., Olesen, N.A., Bak, C., and Kim, T.: Full-scale test of trailing edge flaps on a Vestas V27 wind turbine: active load reduction and system identification, *Journal of Wind Energy*, DOI 10.1002/we.1589, 2013.
- 305 Castaignet, D., Couchman, I., Poulsen, N.K., Buhl, T., and Wedel-Heinen, J.J.: Frequency weighted model predictive control of trailing edge flaps on a wind turbine blade, *IEEE Transactions On Control Systems Technology*, vol.21 No. 4 1105-1116, 2013.
- Castaignet, D., Wedel-Heinen, J., Kim, T., Buhl, T., and Poulsen, N.: Results from the first full scale wind turbine equipped with trailing edge flaps, Proceedings of the 28th AIAA Applied Aerodynamics Conference, AIAA 10.2514/6.2010-4407, Chicago, USA, 2010.
- 310 Couchman, I., Castaignet, D., Poulsen, N.K., Buhl, T., Wedel-Heinen, J.K., and Olesen, N.A.: Active load reduction by means of trailing edge flaps on a wind turbine blade, American Control Conference June 4-6, 2014, Portland, Oregon, USA, 2014.
- Enevoldsen, P.B., and Gomez Gonzalez, A.: Active trailing edge flaps in turbine design - a mature technology?, Proceedings of the TEM87 Smart Blades Expert Meeting IEA Task 11, Copenhagen, 2017.
- Enevoldsen, P.B.: Load validation and advanced modelling, *Advances in Rotor Blades for Wind Turbines - IQPC Conference*, Bremen, Germany, April 24-26, 2018.
- 315 Energiteknologiske Udviklings- of Demonstrationsprogram. Project Journal Nr. 64015-0069.
- Gomez, A., Enevoldsen, P.B., Akay, B., Barlas, T.K., Fischer, A., and Madsen, H.Aa.: Experimental and numerical validation of active flaps for wind turbine blades, *J. Phys.: Conf. Ser.* 1037-022039, DOI :10.1088/1742-6596/1037/2/022039, 2018.
- Holling, M.: Progress on Blades with Adaptative Leading Edges, Proceedings of the TEM87 Smart Blades Expert Meeting IEA Task 11, Copenhagen, 2017.
- 320 Induflap2 project information website. <http://www.induflap.dk>, last access: Feb 3, 2020.

- Frederik, J., Navalkar, S., van Wingerden, J.W., Barlas, T., Madsen, H.A., Olsen, A.S., Andersen, T.L., Lars, L., Riziotis, V., Ai, Q., Weaver, P., Bergami, L. and Kloepfer, J.: Demonstration and validation of new control concepts by dedicated and scaled turbine experiments. INNWind.eu project report WP 2.3.3, 2017.
- 325 Jensen, P.J., Chaviaropoulos, T., and Natarajan, A.: LCOE reduction for the next generation offshore wind turbines. Outcomes from the INNWIND.EU project, 2017.
- Johnson, S. and van Dam, C.P.: Active load control techniques for wind turbines, Sandia National Laboratories, SAND2008-4809, Dept of mech. and aeronautical engineering. University of California. Davis, USA, 2008.
- Madsen, H.A., Barlas, A. and Andersen, T.L.: Testing of a new morphing trailing edge flap system on a novel outdoor rotating test rig, 330 Scientific Proceedings, EWEA Annual Conference and Exhibition, pp. 26-30, 2015.
- Madsen, H.A., Barlas, A. and Andersen, T.L.: A morphing trailing edge flap system for wind turbine blades, Proceedings of the 7th ECCO-MAS Thematic Conference on Smart Structures and Materials, 2015.
- Matsuda, H., Tanaka, M., Osako, T., Yamazaki, K., Shimura, N., Asayama, M., and Oryu, Y.: Plasma Actuation Effect on a MW class Wind Turbine, International Journal of Gas Turbine, Propulsion and Power Systems, vol. 9, nr. 1, 2017.
- 335 General Electric Company: MOD-5A Wind turbine generator program design report. Volume 1 - Executive Summary, NASA CR-174734, Cleveland, USA, 1984.
- Pechlivanoglou, G.: Passive and active flow control solutions for wind turbine blades. Ph.D. Thesis, Technische Universität Berlin, 2013.
- Peña, A., Floors, R., Sathe, A., Gryning, S.E., Wagner, R., Courtney, M., Larsen, X.G., Hahmann, A.N., Hasager, C.B., Ten Years of Boundary Layer and Wind Power Meteorology at Høvsøre, Denmark, Journal of Boundary Layer Meteorology, DOI 10.1007/s10546-015-0079-8, 340 2015.
- Pereira, R.: Smart Rotor Research using DBD Plasma as Flow Control Actuators: an overview of TUDelft's Efforts, Proceedings of the TEM87 Smart Blades Expert Meeting IEA Task 11, Copenhagen, 2017.
- Riemenschneider, J.: Smart Blades - Progress on Blades with Active Trailing Edges, Proceedings of the TEM87 Smart Blades Expert Meeting IEA Task 11, Copenhagen, 2017.
- 345 Rubak R. and Petersen, J.T.: Monopile as Part of Aeroelastic Wind Turbine Simulation Code, Proceedings of Copenhagen Offshore Wind 2005.
- Samara, F. and Johnson, D.A.: In-blade Load Sensing on 3D Printed Wind Turbine Blades Using Trailing Edge Flaps, J. Phys.:Conf. Ser. vol. 1037-052023, 2018.
- Samara, F. and Johnson, D.A.: In-Blade Measurements of Cyclic Loading on Yawed Turbines with Trailing Edge Flap, J. Phys.:Conf. Ser. 350 vol 1452-012061, 2020.
- Skjoldan, P.F.: Aeroelastic modal dynamics of wind turbines including anisotropic effects. Ph.D. Thesis, DTU Risoe-PhD-66, 2011.
- TEM 87 Smart Blades Proceedings. Roskilde, DK 2017, Homepage of the TEM communities of IEA Task 11 <https://community.ieawind.org/task11/ourlibrary> , TEM 87 Smart Structures for Large Wind Turbine Rotor Blades, last access: Aug 23, 2020.
- 355 Pechlivanoglou, G., Fischer, J., Eisele, O., Vey, S., Nayeri, C.N. and Paschereit, C.O.: Development of a medium scale research HAWT for inflow and aerodynamic research in the TU Berlin wind tunnel, Proceedings of German Wind Energy Conference DEWEK2015, 2017.